Supplemental Materials for

# Succinate dehydrogenase/complex II is critical for metabolic and epigenetic regulation of T cell proliferation and inflammation

Xuyong Chen *et al.*

*Correspondence should be addressed to:

**Ruoning Wang,** Phone: 614-335-2980; Fax: 614-722-5895.

ruoning.wang@nationwidechildrens.org;

**Teresa W.-M. Fan,** Phone: 858-218-1028, Fax: 859-257-1307.

twmfan@gmail.com;

**Benjamin Stanton,** Phone: 614-355-2691; Fax: 614-722-5895.

Benjamin.Stanton@nationwidechildrens.org;

**Supplemental Materials**

Figs. S1 to S15
Tables S1 to S5
Data file S1

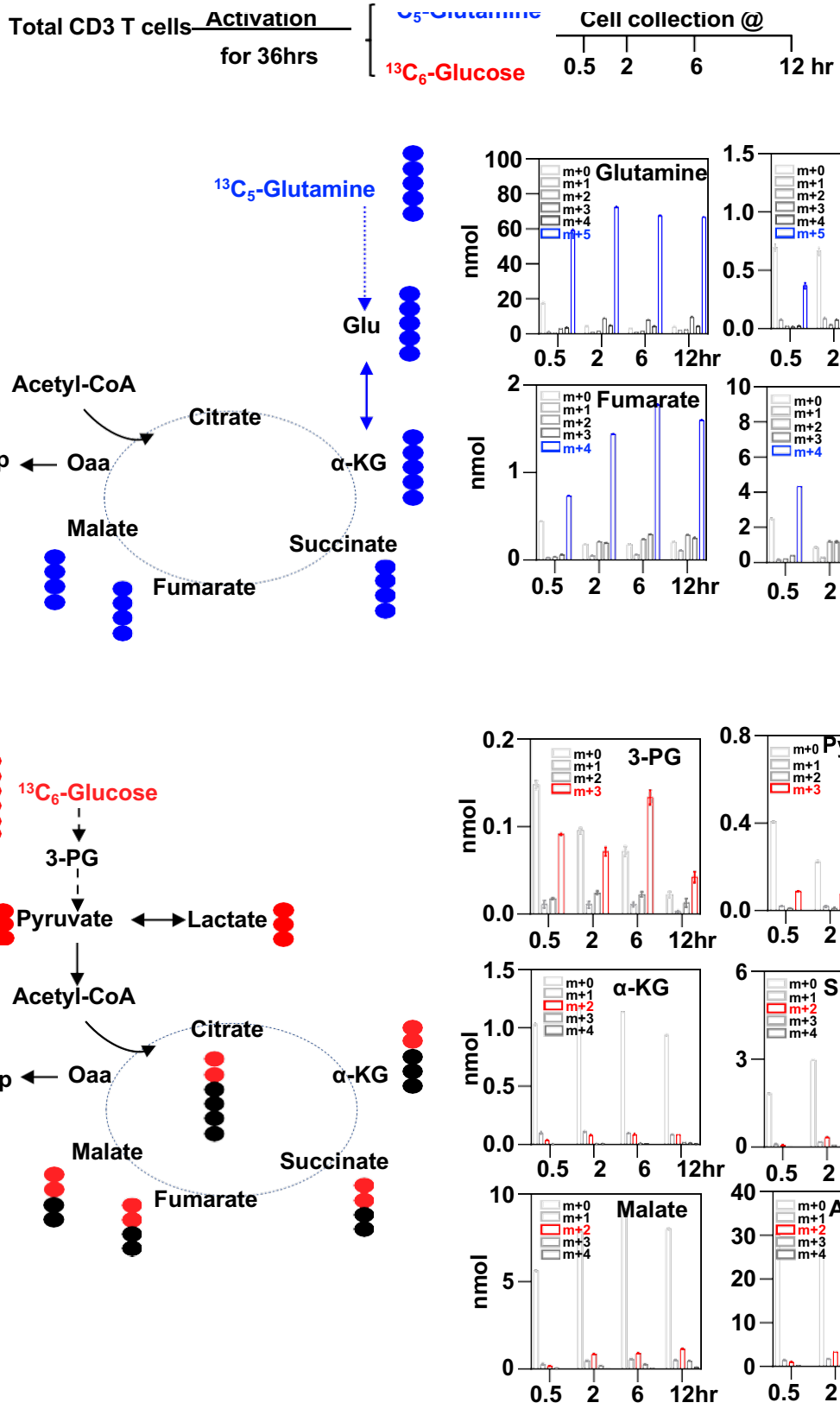


upplemental figure 1. The TCA cycle allocates carbon input from glucose nd glutamine to support T cell growth and proliferation.

**Supplemental figure 1. The TCA cycle allocates carbon input from glucose and glutamine to support T cell growth and proliferation.**

**(A)** The experimental procedure of isotope $^{13}C_5$-Glutamine and $^{13}C_6$-Glucose labeling and metabolite quantification by GC-MS. **(B-C)** Diagram of putative catabolic routes of $^{13}C_5$-Glutamine (**B**) or $^{13}C_6$-Glucose (**C**) in T cells (left panel), quantification results were present in the right panel, numbers in the X-axis represent indicated time points, bar with different colors represent those of $^{13}C$ atoms in given metabolites, numbers in the Y-axis represent the levels of the metabolites (nmol). n=3, one experiment, bar graphs, mean ± SEM.

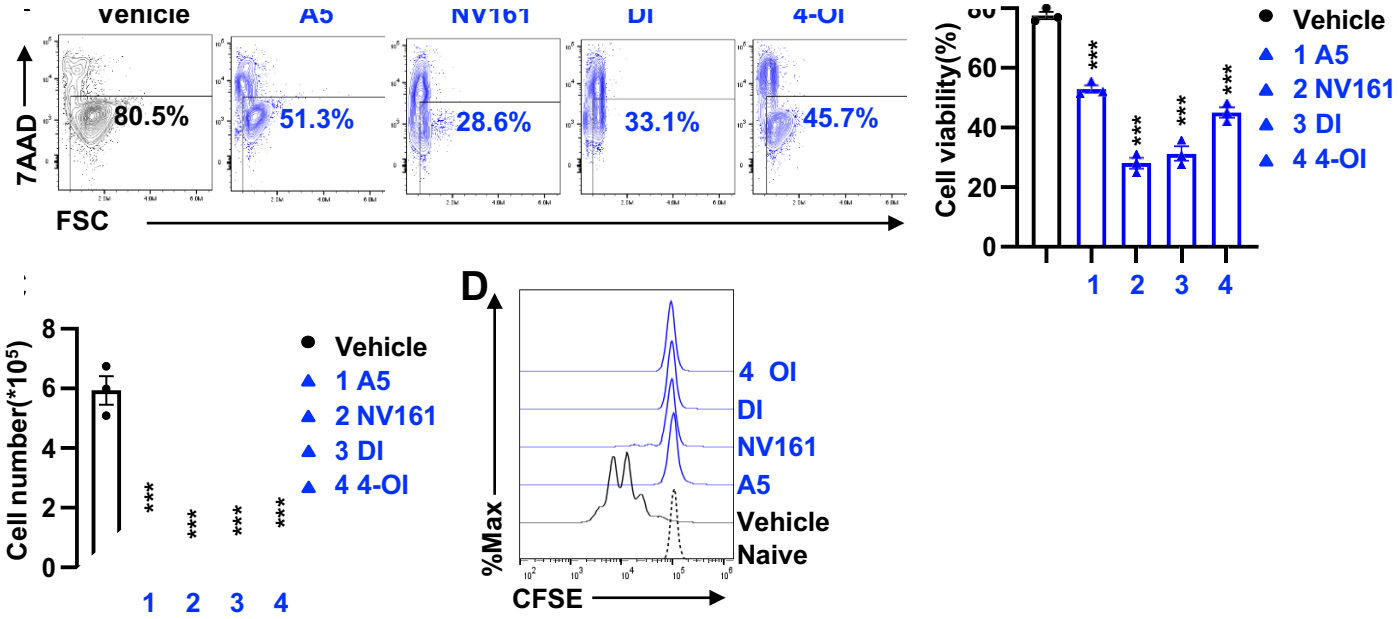


**Supplemental figure 2. Complex II is required for T cell growth and proliferation.**

**Supplemental figure 2. Complex II is required for T cell growth and proliferation.**

**(A-D)** WT $CD4^+$ T cells were activated with indicated treatments (atpenin A5 (A5, 100nM), diacetoxymethyl malonate (NV161,100μM), dimethyl-itaconate (DI, 0.5mM), or 4-octyl-itaconate (4OI, 500μM)) for 72 hrs, cell viability was assessed by 7AAD uptake **(A, B)**, cell number was calculated by a cell counter **(C)**, cell proliferation was determined by CFSE dilution **(D)**. n=3, data are representative of 3 independent experiments, ***$p < 0.001$, one-way ANOVA. T cells were activated by the plate-bound anti-CD3/CD28 antibodies.

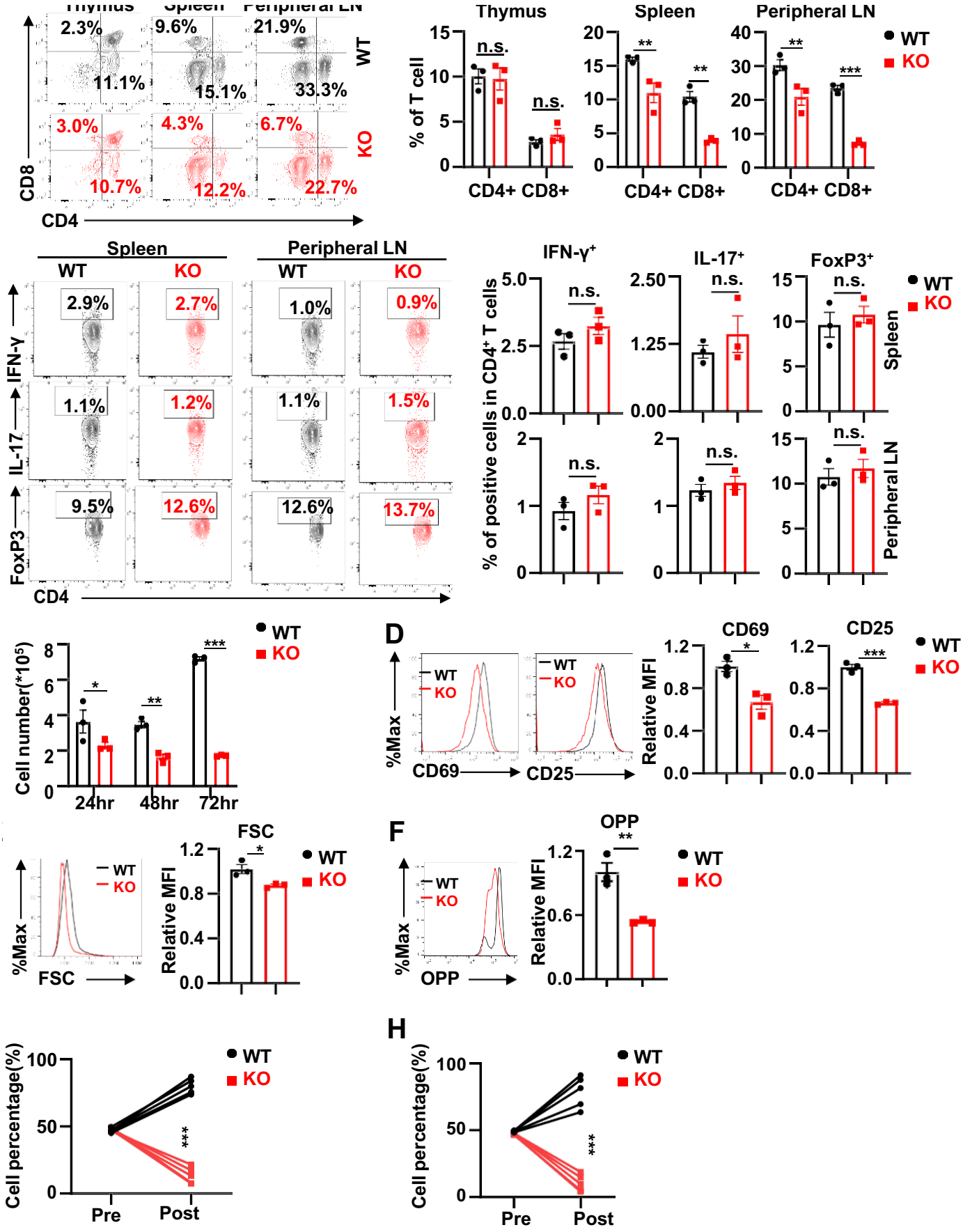


**Supplemental figure 3. Complex II/SDHB is required for T cell development and activation.**

**Supplemental figure 3. Complex II/SDHB is required for T cell development and activation.** **(A-B)** Distribution of indicated T cell subsets in the thymus, spleen, and peripheral lymph node (LN) were determined by cell surface and intracellular markers by flow cytometry. n=3, data are representative of 3 independent experiments, n.s., not significant, $**p < 0.01$, $***p < 0.001$, two-way ANOVA, student's *t* test. (**C**) Cell numbers of the indicated $CD4^+$ T cells were measured by a cell counter, n=3, data are representative of 3 independent experiments, $*p < 0.05$, $**p < 0.01$, $***p < 0.001$, one-way ANOVA. **(D-F)** Cell surface markers (CD69 and CD25), size (FSC), protein contents (OPP) of the indicated cells (24 h after activation) were determined by flow cytometry, n=3, data are representative of 3 independent experiments, $*p < 0.05$, $**p < 0.01$, $***p < 0.001$, student's *t* test. T cells (C-F) were activated by the plate-bound anti-CD3/CD28 antibodies. **(G-H)** $CD4^+$ T cell ratios of *in vivo* competitive proliferation (**G**) or antigen-specific competitive proliferation (**H**) before (Pre) and after (Post) adoptive transfer were determined by surface staining of isogenic markers, n=5, data are representative of 3 independent experiments, $***p < 0.001$, two-way ANOVA. Bar graphs, mean ± SEM.

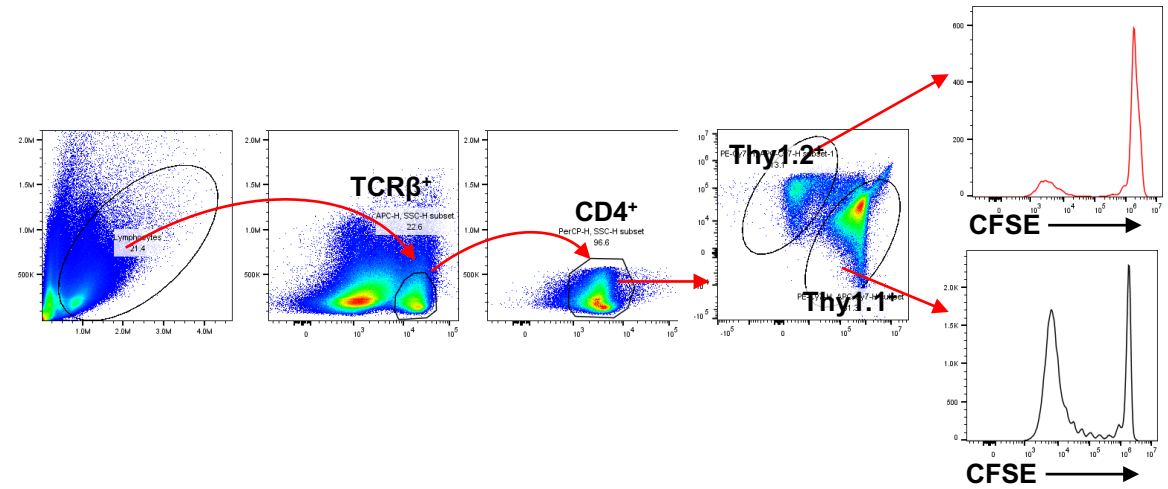


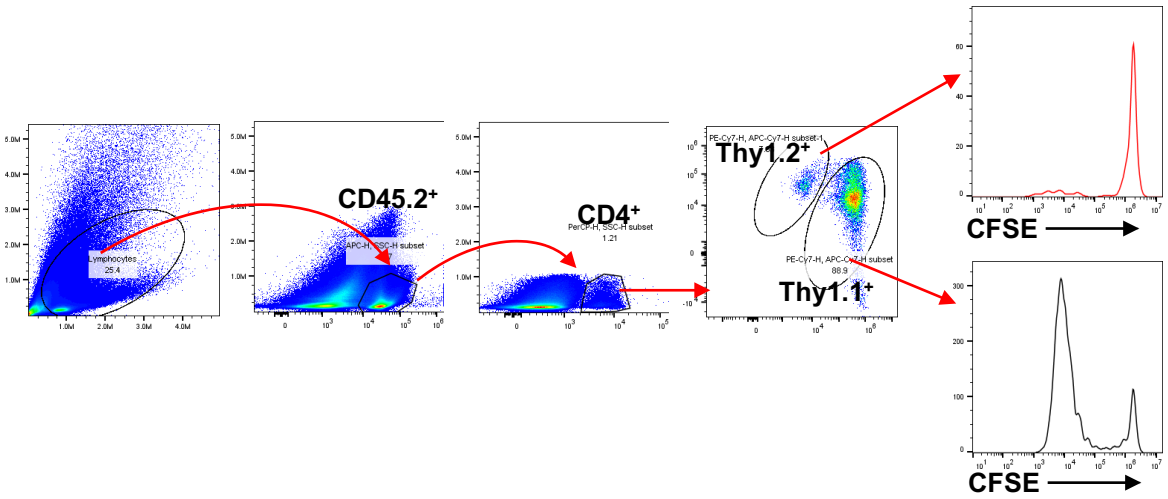


**upplementary figure 4. Gating strategies applied in homeostatic (A) or ntigen-specific (B) proliferation assays (Related to Figure. 1G-H).**

**Supplementary figure 4. Gating strategies applied in homeostatic or antigen-specific proliferation assays (Related to Figure 1. G-H).**

**(A)** Lymph nodes were harvested from lymphopenic host mice (*Rag*$^{-/-}$), and processed into single-cell suspensions. The donor T cells were gated from TCRβ$^{+}$CD4$^{+}$ cells and parsed by Thy1.1(WT) and Thy1.2(*SDHB* cKO), cell proliferation was determined by CFSE dilution, related to figure 1G.

**(B)** Lymph nodes were harvested from CD45.1$^{+}$ host mice, and processed into single-cell suspensions. The donor T cells were gated from CD45.2$^{+}$CD4$^{+}$ cells and parsed by Thy1.1(WT) and Thy1.2(*SDHB* cKO), cell proliferation was determined by CFSE dilution, related to figure 1H.

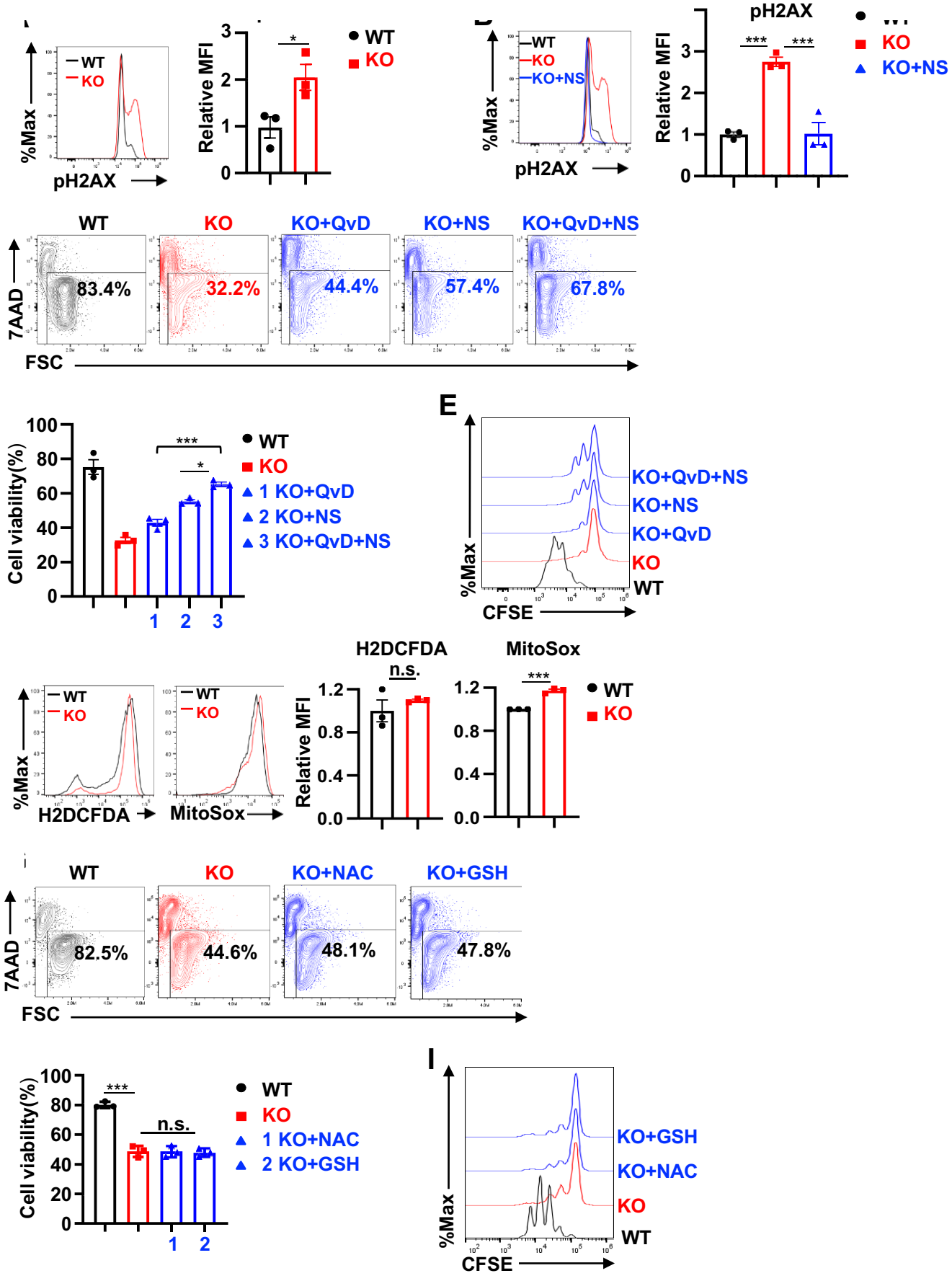


upplemental figure 5. SDHB deficiency induces DNA damage and moderately ıcreases ROS production.

**Supplemental figure 5. SDHB deficiency induces DNA damage and moderately increases ROS production.**

**(A-B**) $CD4^+$ T cells were activated for 24 hrs with indicated treatment, DNA damage was determined by staining phosphor-Histone H2A.X(Ser139) by flow cytometry, n=3, data are representative of 2 independent experiments, $*p < 0.05$, $***p < 0.001$, student's *t* test, one-way ANOVA. **(C-E)** $CD4^+$ T cells were activated for 72 hrs with indicated treatments, cell viability was determined by 7AAD uptake **(C-D)**, cell proliferation was determined by CFSE dilution **(E)**, n=3, data are representative of 2 independent experiments, $*p < 0.05$, $***p < 0.001$, one-way ANOVA. (**F**) $CD4^+$ T cells were activated for 24 hrs, intracellular ROS and mitochondrial ROS were measured by the H2DCFDA staining or MitoSOX™ Red staining by flow cytometry, n.s., not significant, $***p < 0.001$, student's *t* test. **(G-I)** $CD4^+$ T cells were activated for 72 hrs with indicated treatments. Cell viability was determined by 7AAD uptake **(G-H)**, cell proliferation was determined by CFSE dilution **(I)**, n=3, data are representative of 2 independent experiments, n.s., not significant, $***p < 0.001$, one-way ANOVA. Bar graphs, mean ± SEM. T cells were activated by the plate-bound anti-CD3/CD28 antibodies.

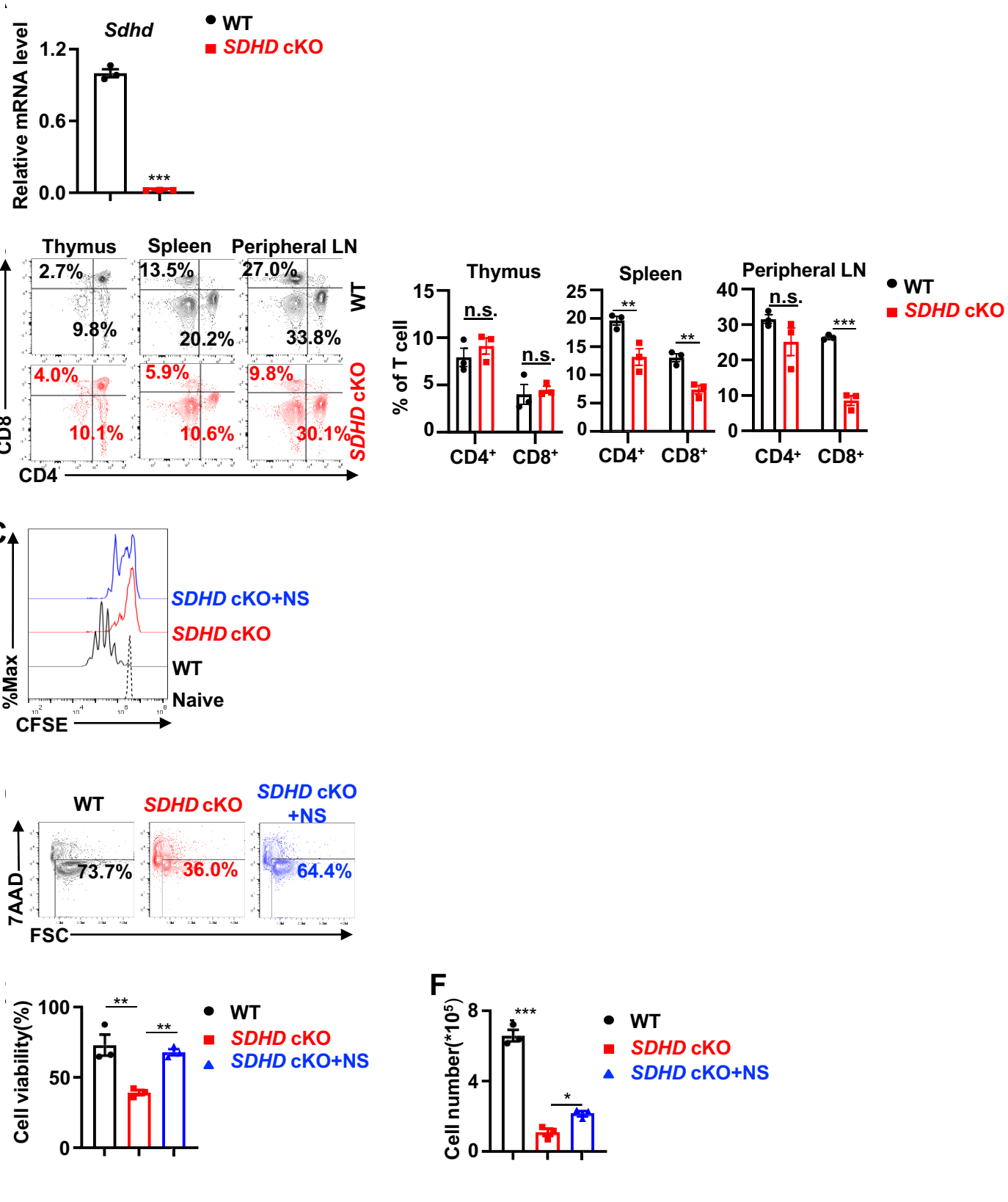


Supplemental figure 6. SDHD deficiency phenocopies SDHB deficiency in T cell.

**Supplemental figure 6. SDHD deficiency phenocopies SDHB deficiency in T cell.**

**(A)** SDHD mRNA levels of the indicated T cells were determined by qPCR (n=3), ***$p < 0.001$, student's *t* test. **(B)** Distribution of indicated T cell subsets in the thymus, spleen, and peripheral lymph node (LN) were determined by cell surface markers by flow cytometry, n=3, data are representative of 3 independent experiments, n.s., not significant, *$p < 0.05$, **$p < 0.01$, ***$p < 0.001$, one-way ANOVA. **(C-F)** $CD4^+$ T cells were activated by the plate-bound anti-CD3/CD28 antibodies for 72 hrs with indicated treatment, cell proliferation was determined by CFSE dilution **(C)**, cell viability was determined by 7AAD uptake **(D-E)**, and cell number was measured by a cell counter **(F).** n=3, data are representative of 3 independent experiments, *$p < 0.05$, **$p < 0.01$, ***$p < 0.001$, one-way ANOVA. Bar graphs, mean ± SEM.

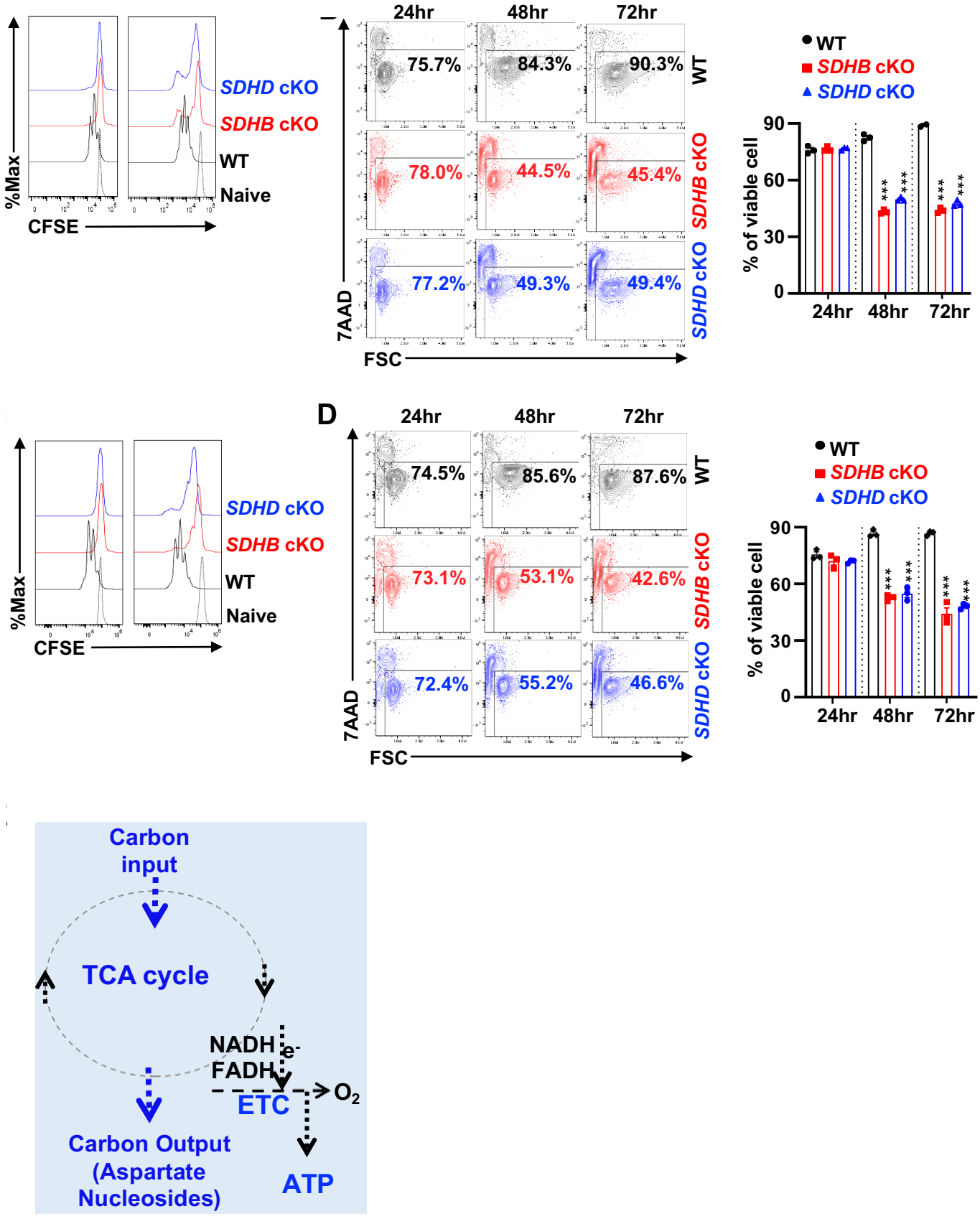


upplemental figure 7. SDHB or SDHD deficiency suppresses cell proliferation nd survival during differentiation.

**Supplemental figure 7. SDHB or SDHD deficiency suppresses cell proliferation and survival during differentiation.**

(**A-D**) $CD4^+$ T cells were polarized under $T_H1$ **(A and B)** and $T_H17$ **(C and D)** differentiation conditions, cell proliferation was determined by CFSE dilution (**A and C**), cell viability was determined by 7AAD uptake (**B and D**), n=3, data are representative of 3 independent experiments, ***$p < 0.001$, one-way ANOVA. **(E)** Schematic view of carbon input and output through the TCA cycle. Bar graphs, mean ± SEM.

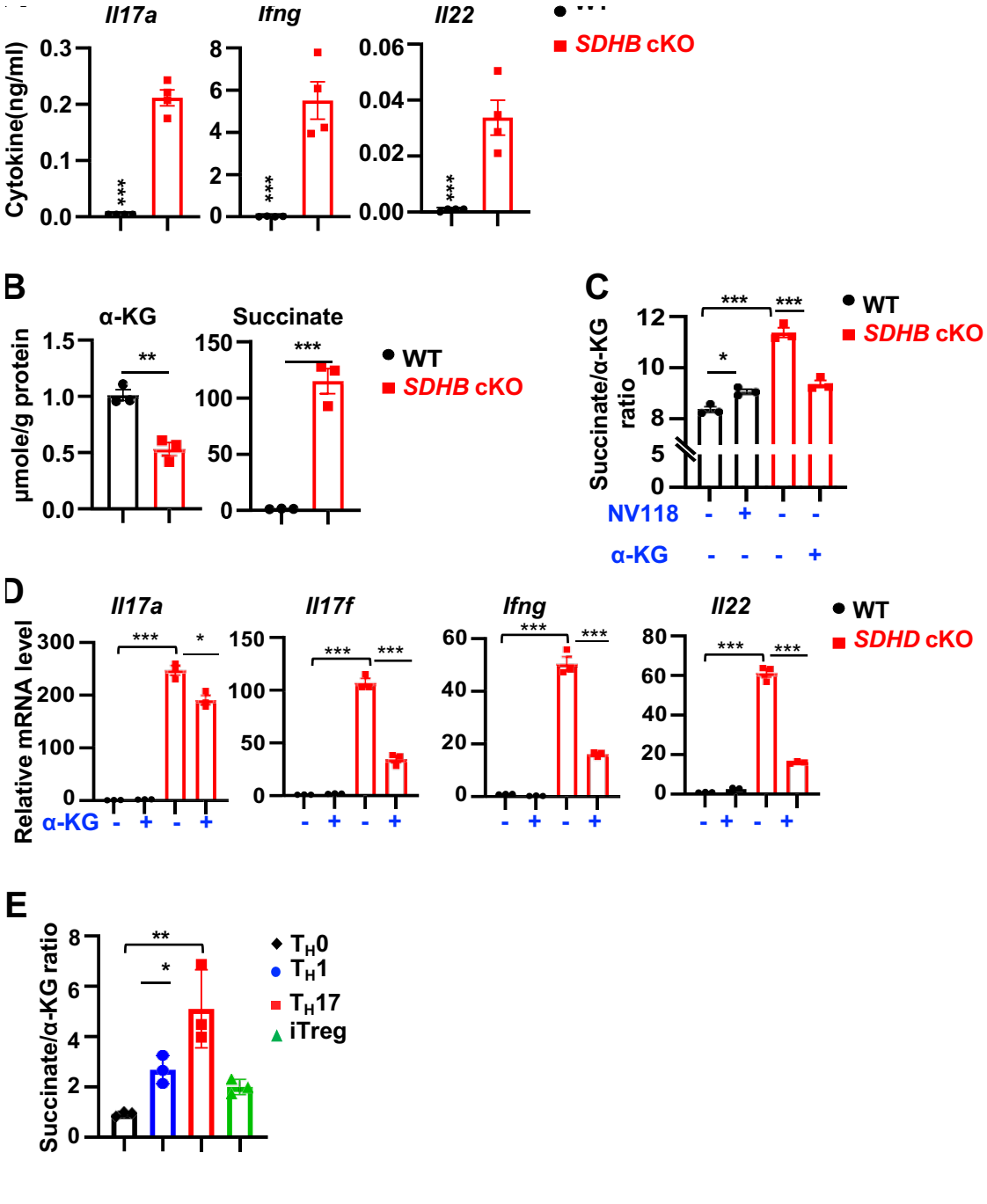


**Supplemental figure 8. Increasing the succinate/α-KG ratio promotes T cell inflammation.**

**Supplemental figure 8. Increasing the succinate/α-KG ratio promotes T cell inflammation.**

**(A)** Indicated cytokines were measured by the LEGEND plex™ kits by flow cytometry, n=4 from one experiment, ***$p < 0.001$, Student's *t* test. **(B)** Metabolites of the indicated T cells were extracted and analyzed using IC-UHR-FTMS, n=3 from one experiment, **$p < 0.01$, ***$p < 0.001$, student's *t* test**. (C)** The succinate and α-KG levels from naïve T cells with indicated treatment and genotypes were measured using colorimetric assay kits, n=3 from one experiment, *$p<0.05$, ***$p<0.001$, one-way ANOVA**. (D)** CD4 T cells were activated for 36 hrs with or without 10mM α-KG, mRNA levels of indicated genes were measured by qPCR, n=3, data are representative of 3 independent experiments, *$p < 0.05$, ***$p < 0.001$, one-way ANOVA. (**E**) Metabolites of the indicated T cells were extracted and analyzed using IC-UHR-FTMS, n=3 from one experiment, *$p<0.05$, **$p<0.01$, one-way ANOVA**.** Bar graphs, mean ± SEM. $CD4^+$ T cells were activated by the plate-bound anti-CD3/CD28 antibodies (A, B and D) or polarized toward the indicated T cell lineages (E)

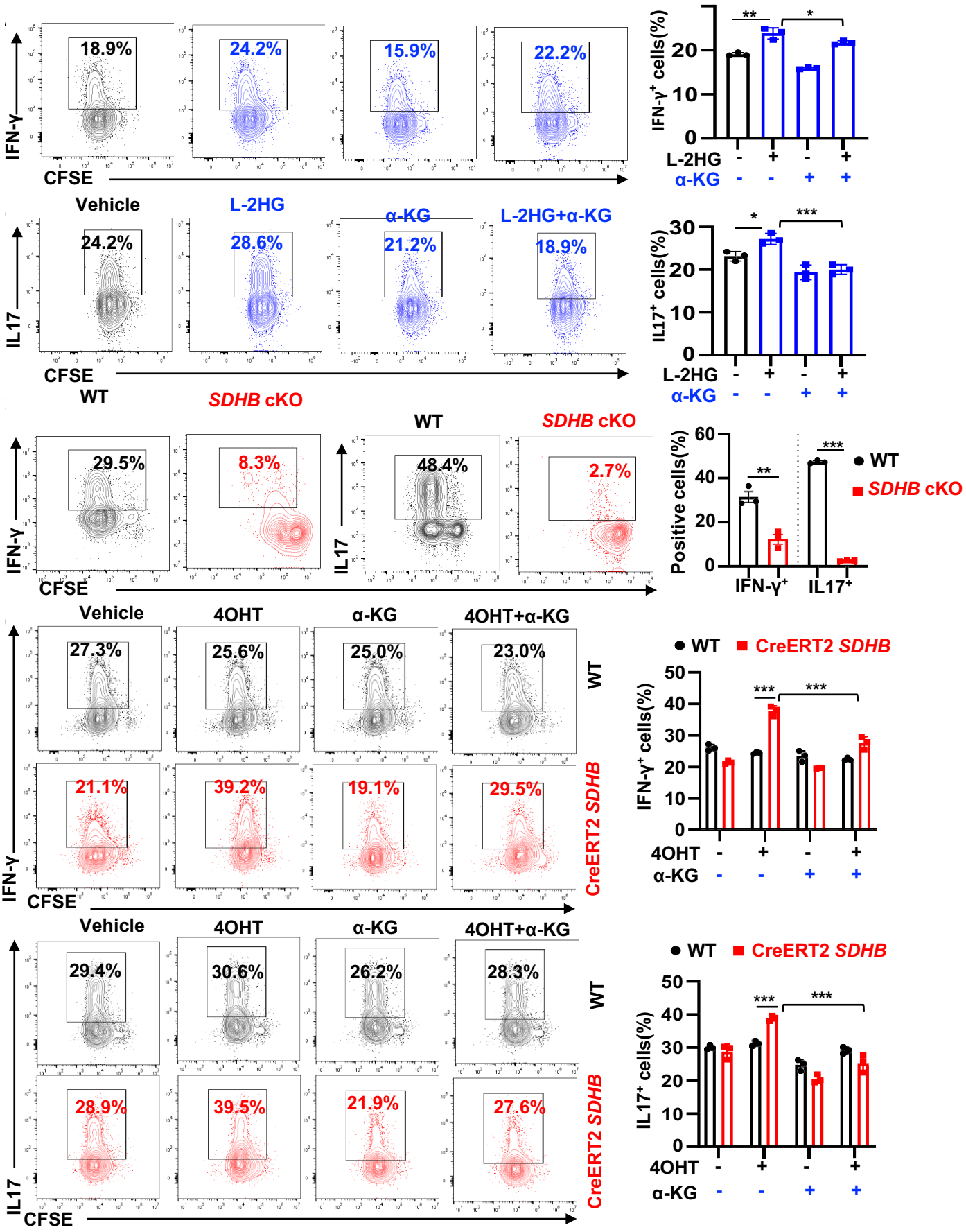


**Supplemental figure 9. Acute deletion of SDHB enhances $T_H1$ and $T_H17$ differentiation.**

**Supplemental figure 9. Acute deletion of SDHB enhances $T_H1$ and $T_H17$ differentiation.**

**(A-E)** $CD4^+$T cells were polarized under $T_H1$ and $T_H17$ differentiation conditions with indicated treatment (1μM L-2HG, 2mM α-KG, 600nM 4OHT) for 72 hrs. The indicated proteins were quantified by intracellular staining. Cell proliferation was determined by CFSE staining. n=3, data are representative of 2 independent experiments, *$p$<0.05, **$p$<0.01, ***$p$<0.001, student's *t-test*, one-way ANOVA, two-way ANOVA. Bar graphs, mean ± SEM.

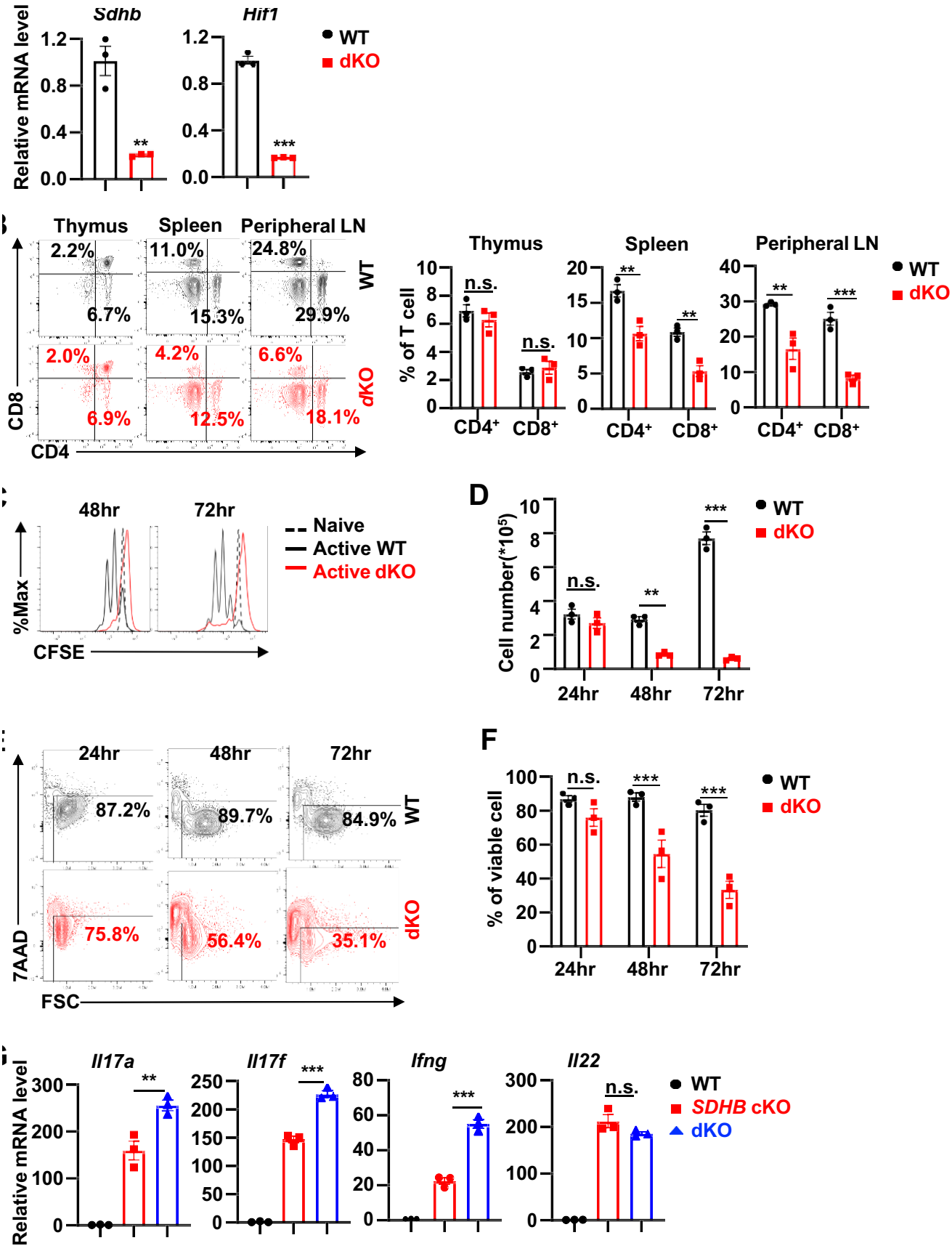


**Supplemental figure 10. HIF1-α is dispensable for pro-inflammatory gene signature caused by SDHB deficiency.**

**Supplemental figure 10. HIF1-$\alpha$ is dispensable for pro-inflammatory gene signature caused by SDHB deficiency.**

**(A)** mRNA levels of indicated genes were measured by the qPCR (n=3), $^{**}p<0.01$, $^{***}p<0.001$, student's *t* test. **(B)** Distribution of indicated T cell subsets in the thymus, spleen, and peripheral lymph node (LN) were determined by cell surface markers by flow cytometry, n=3, data are representative of 3 independent experiments, n.s., not significant, $^{**}p < 0.01$, $^{***}p < 0.001$, two-way ANOVA. **(C-G)** The indicated $CD4^+$ T cells were activated by the plate-bound anti-CD3/CD28 antibodies for the indicated times. Cell proliferation was determined by CFSE dilution (**C**), cell number was determined by the cell counter **(D)**, cell viability was determined by 7AAD uptake **(E, F)**, mRNA levels of indicated genes were determined by qPCR **(G)**, n=3, data are representative of 3 independent experiments, n.s., not significant, $^{**}p < 0.01$, $^{***}p < 0.001$, one-way ANOVA.

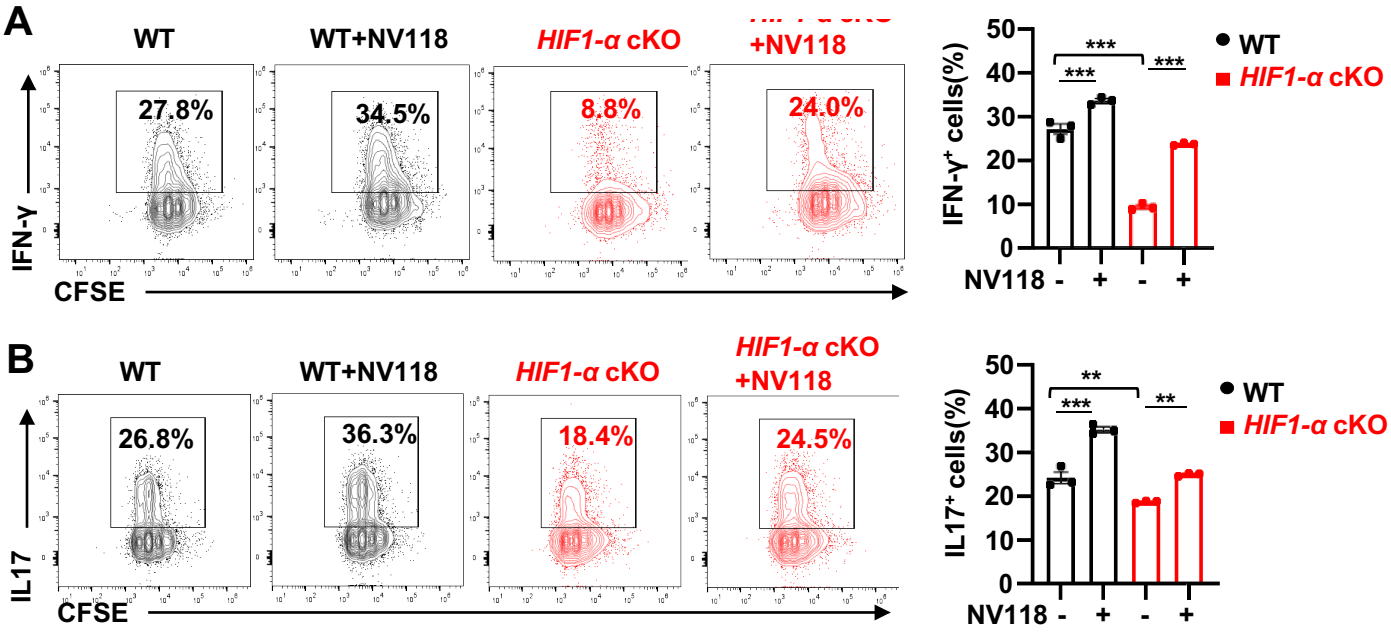


**Supplemental figure 11. HIF1-α is dispensable for pro-inflammatory gene signature caused by succinate accumulation.**

**Supplemental figure 11. HIF1-$\alpha$ is dispensable for pro-inflammatory gene signature caused by succinate accumulation.**

**(A-B)** $CD4^+$ T cells were polarized toward $T_H1$ **(A)** and $T_H17$ **(B)** lineages with indicated treatment (25 μM NV118) for 72 hrs. The indicated proteins were quantified by intracellular staining by flow cytometry. Cell proliferation was determined by CFSE staining, n=3, data are representative of 2 independent experiments, $^{**}p < 0.01$, $^{***}p < 0.001$, one-way ANOVA. Bar graphs, mean ± SEM.

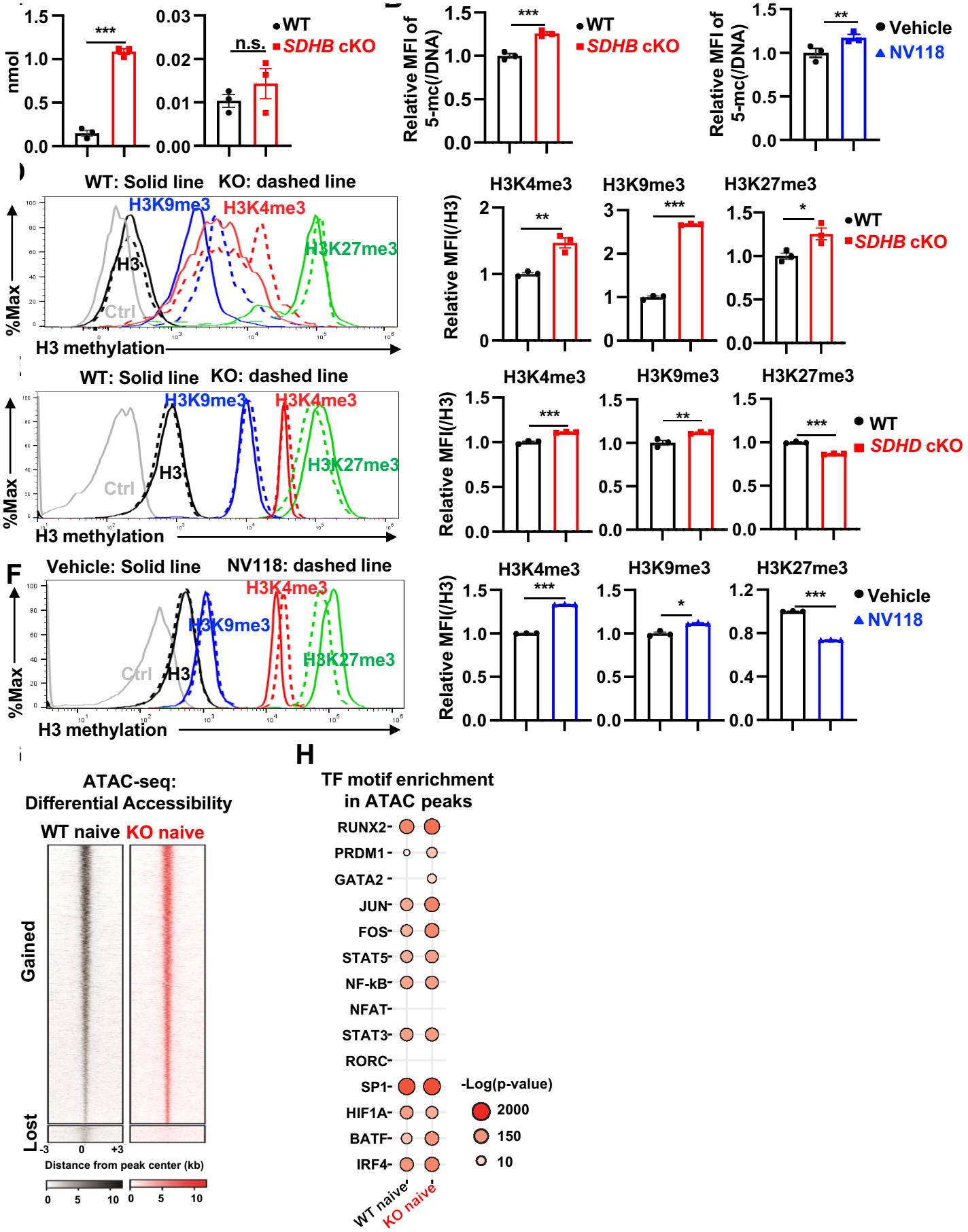


**Supplemental figure 12. Succinate accumulation impacts T cell epigenome.**

**Supplemental figure 12. Succinate accumulation impacts T cell epigenome.**

**(A)** Indicated metabolites in naive T cells were determined by GC-MS, n=3 from one experiment, n.s., not significant, ***$p$<0.001, student's $t$ test. **(B-C)** DNA methylation levels in naive T cells with indicated genotypes or treatment were determined by 5-mc staining by flow cytometry. **(D-F)** Indicated histone methylation levels in naive T cells with indicated genotypes or treatment were determined by intracellular staining by flow cytometry (gray line represented isotope ctrl, black line represented total H3, blue line represented H3K9me3, red line represented H3K4me3, green line represented H3K27me3, solid line represented WT, dashed line represented KO or NV118 treatment), n=3, data are representative of 3 independent experiments, *$p$<0.05, **$p$<0.01, ***$p$<0.001, student's $t$ test. (**G**) Differential chromatin accessibility was measured by ATAC-seq in naïve CD4 T cells between indicated genotypes (n = 3 replicates for each genotype), identifying 5,086 sites with accessibility gain and 346 sites with accessibility loss in *SDHB* cKO T cells. (**H**) Motif analysis was performed in differential ATAC-seq peaks (WT vs. *SDHB* cKO naïve CD4 T cells), identifying motif enrichment for transcription factors involved in T cell activation and inflammation.

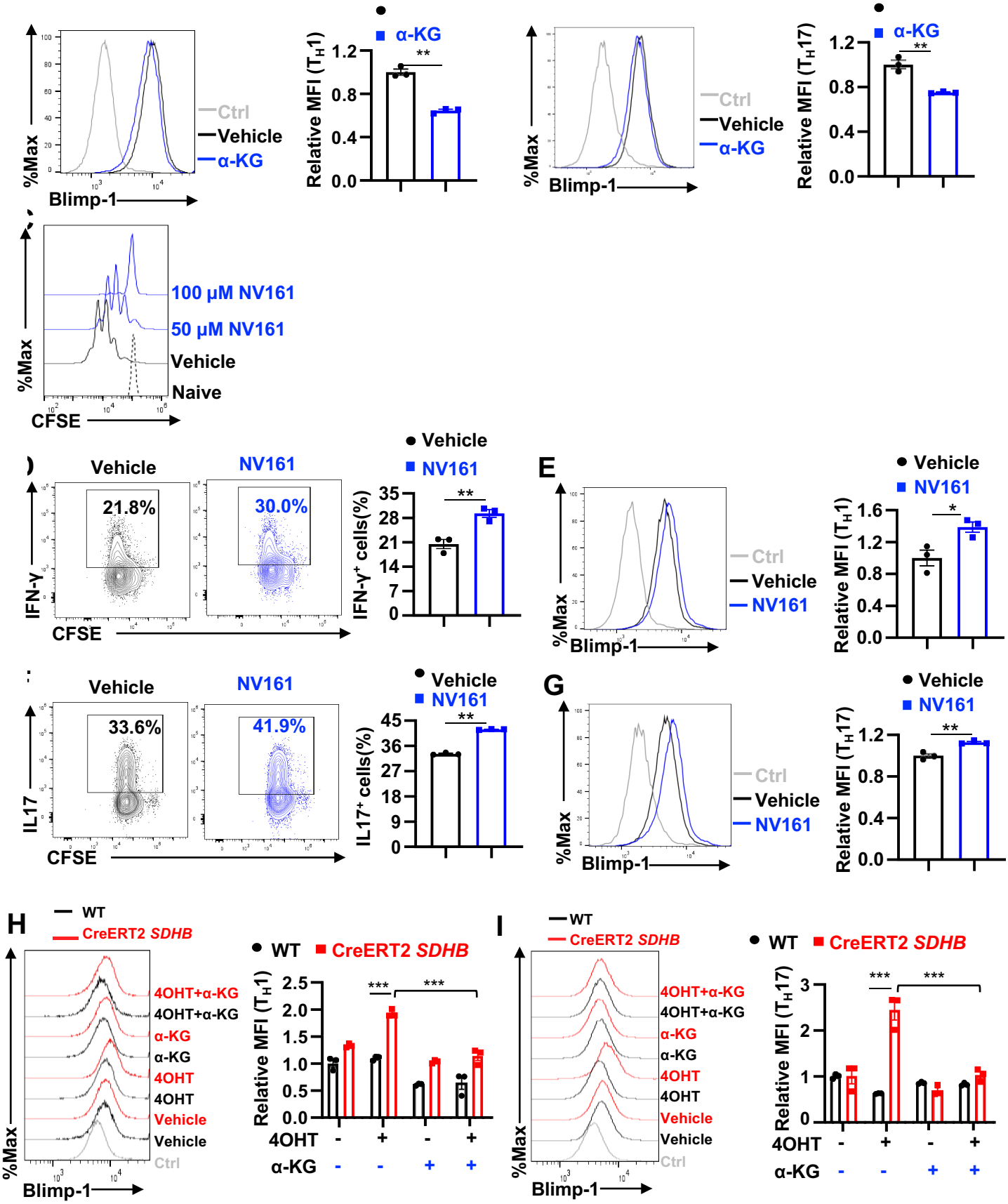


**Supplemental figure 13. Changing the succinate/α-KG ratio affects *Kdm1*/Blimp-1 expression during T cell differentiation.**

**Supplemental figure 13. Changing the succinate/α-KG ratio affects *Prdm1*/Blimp-1 expression during T cell differentiation.**

**(A-I)** $CD4^+$T cells were polarized toward $T_H1$ (A, D, E and H) and $T_H17$ (B, F, G and I) lineages with indicated treatment (2mM α-KG, 50μM NV161, 600nM 4OHT) for 72 hrs. The indicated proteins were quantified by intracellular staining by flow cytometry. Cell proliferation was determined by CFSE staining (**C**). n=3, data are representative of 3 independent experiments, *$p$<0.05, **$p$<0.01, ***$p$<0.001, student's *t-test*, two-way ANOVA. Bar graphs, mean ± SEM.

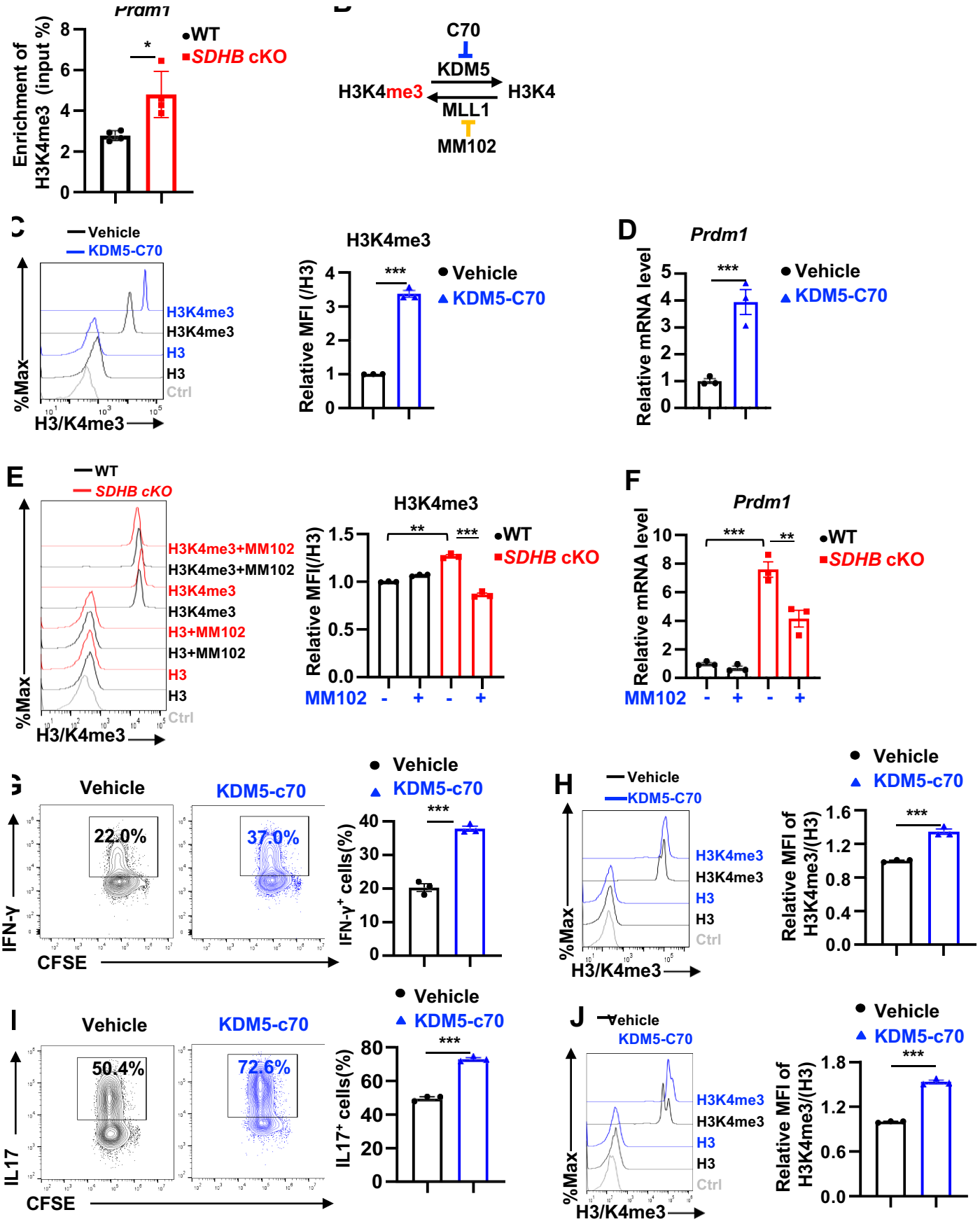


**Supplemental figure 14. Changing the succinate/α-KG ratio affects *Prdm1*/Blimp-1 expression through modulating the level of H3K4me3.**

**Supplemental figure 14. Changing the succinate/α-KG ratio affects *Prdm1*/Blimp1 expression through modulating the level of H3K4me3.**

**(A)** The enrichment of H3K4me3 at the promoter of *Prdm1* was measured by the ChIP-qPCR, n=4 replicates for each genotype, **p*<0.05, student's *t-test*. (**B)** The diagram of KDM5-C70 and MM102 on regulating H3K4 trimethylation. (**C-F)** $CD4^+$ T cells were maintained in naïve condition with 25μM MM102 for 48 hrs or 10μM KDM5-C70 for 72 hrs, H3K4me3 levels were measured by intracellular staining by flow cytometry (C and E); the cells were then activated by the plate-bound anti-CD3/CD28 antibodies for 36 hrs, and mRNA levels of *Prdm1* were measured by qPCR (D and F), n=3, data are representative of 3 independent experiments, ***p*<0.01, ****p*<0.001, student's *t* test, one-way ANOVA. **(G-J)** $CD4^+$T cells were polarized toward $T_H1$ (G and H) and $T_H17$ (I and J) lineages with 5μM KDM5-C70 for 72 hrs. The indicated proteins were quantified by intracellular staining by flow cytometry. Cell proliferation was determined by CFSE staining. n=3, data are representative of 3 independent experiments, ****p*<0.001, student's *t-test*. Bar graphs, mean ± SEM.

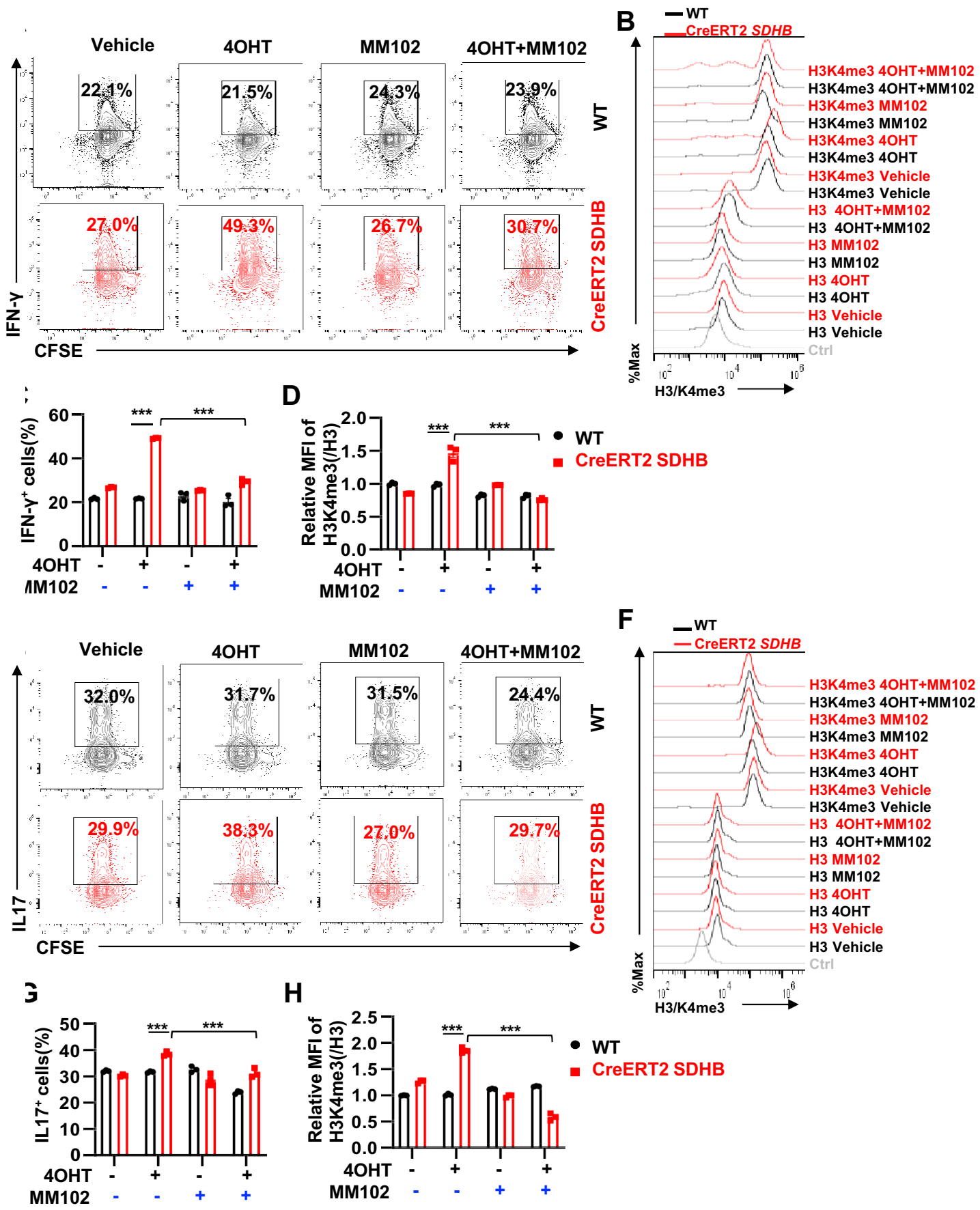


**upplemental figure 15. Changing the succinate/α-KG ratio regulates *rdm1*/Blimp-1 expression through an epigenetic mechanism.**

**Supplemental figure 15. Changing the succinate/α-KG ratio regulates *Prdm1*/Blimp-1 expression through an epigenetic mechanism.**

**(A-H)** $CD4^+$T cells were polarized toward $T_H1$ (A-D) and $T_H17$ (E-H) lineages with indicated treatment (10μM MM102, 600nM 4OHT) for 72 hrs. The indicated proteins were quantified by intracellular staining by flow cytometry. Cell proliferation was determined by CFSE staining. n=3, data are representative of 3 independent experiments, ***$p$<0.001, two-way ANOVA. Bar graphs, mean ± SEM.

**Supplemental Table 1. Cell culture-related antibodies, cytokines, inhibitors, chemicals**

| Name | Cat# | Vendor |
|---|---|---|
| InVivoMAb anti-mouse CD3 | BE0001-1 | BioXcell |
| InVivoMAb anti-mouse CD28 | BE0015-1 | BioXcell |
| InVivoMAb anti-mouse IFNγ | BE0055 | BioXcell |
| InVivoMAb anti-mouse IL-4 | BE0045 | BioXcell |
| InVivoMAb anti-mouse IL-2 | BE0043 | BioXcell |
| Recombinant Murine IL-12 p70 | 210-12 | Peprotech |
| Recombinant Mouse IL-2 | 212-12 | Peprotech |
| Recombinant Murine IL-7 | 217-17 | Peprotech |
| Recombinant Murine IL-6 | 216-16 | Peprotech |
| Recombinant Human TGF-β1 | 100-21C | Peprotech |
| Adenosine | AC164040050 | Thermo Fish Scientific |
| Uridine | U3003 | Sigma-Aldrich |
| Inosine | I4125 | Sigma-Aldrich |
| Cytidine | C4654 | Sigma-Aldrich |
| Guanosine | G6264 | Sigma-Aldrich |
| Thymidine | T1895 | Sigma-Aldrich |
| Q-VD-OPH(QvD) | 1135695-98-5 | BOC science |
| Atpenin A5 | 119509-24-9 | Cayman |
| polyketides NV161 | Cpd ID 01-161-S2; Vial ID BION10476 | Isomerase therapeutics Ltd. Cambridge |
| polyketides NV118 | Cpd ID 01-118-s3; Vial ID BION10474 | Isomerase therapeutics Ltd. Cambridge |
| Dimethyl itaconate | 592498 | Sigma-Aldrich |
| 4-octyl-itaconate | 3133-16-2 | Sigma-Aldrich |
| Dimethyl 2-oxoglutarate (Dim α-KG) | 349631 | Sigma-Aldrich |
| (Z)-4-Hydroxytamoxifen(4OHT) | 68047-06-3 | Sigma-Aldrich |
| GDH1 Inhibitor, R162 - Calbiochem | 5380980001 | Sigma-Aldrich |
| NAC | A7250 | Sigma-Aldrich |
| Glutathione reduced ethyl ester (GSH EE) | G1404 | Sigma-Aldrich |
| MM102 | S7265 | Selleckchem |
| KDM5-C70 | HY-120400 | MedChemExpress |
| (2S)-2-Hydroxyglutaric Acid Octyl Ester Sodium Salt | H942596 | Toronto Research Chemicals |

**Supplemental Table 2. Cell staining antibodies and dyes**

| Name | Cat# | Vendor |
|---|---|---|
| Pacific Blue™ anti-mouse CD4 Antibody | 100428 | BioLegend |
| APC anti-mouse CD4 Antibody | 100516 | BioLegend |
| PE/Cyanine7 anti-mouse CD4 Antibody | 100422 | BioLegend |
| Percp anti-mouse CD4 Antibody | 100432 | BioLegend |
| APC/Cyanine7 anti-mouse CD8a Antibody | 100714 | BioLegend |
| APC anti-mouse TCR β chain Antibody | 109211 | BioLegend |
| PE/Cyanine7 anti-mouse CD90.1 (Thy-1.1) Antibody | 202518 | BioLegend |
| APC/Cyanine7 anti-mouse CD90.2 Antibody | 105328 | BioLegend |
| APC anti-mouse CD90.2 (Thy-1.2) Antibody | 140311 | BioLegend |
| PE/Cyanine7 anti-mouse CD45.1 Antibody | 110730 | BioLegend |
| APC/Cyanine7 anti-mouse CD45.2 Antibody | 109824 | BioLegend |
| FITC anti-mouse CD3 Antibody | 100204 | BioLegend |
| PE-Cy™7 Hamster Anti-Mouse CD69 | 552879 | BD Pharmingen™ |
| CD25 Monoclonal Antibody (PC61.5), PE | 12-0251 | eBioscience™ |
| APC anti-mouse IFN-γ Antibody | 505810 | BioLegend |
| PE/Cyanine7 anti-mouse IFN-γ Antibody | 505826 | BioLegend |
| APC anti-mouse IL-17A Antibody | 506916 | BioLegend |
| PE/Cyanine7 anti-mouse IL-17A Antibody | 506922 | BioLegend |
| Alexa Fluor® 488 Donkey anti-rabbit IgG Antibody | 406416 | BioLegend |
| Alexa Fluor® 647 Donkey anti-rabbit IgG Antibody | 406414 | BioLegend |
| PE/Cyanine7 anti-H2A.X Phospho (Ser139) Antibody | 613419 | BioLegend |
| Alexa Fluor® 647 anti-mouse FOXP3 Antibody | 126407 | BioLegend |
| Anti-5-methylcytosine (5-mC) Antibody (APC) | AC16-0073-03 | Abcore |
| Blimp-1 Monoclonal Antibody (5E7), Alexa Fluor 488 | 53-9850-82 | eBioscience™ |
| Tri-Methyl-Histone H3 (Lys4) (C42D8) Rabbit mAb | 9751 | Cell Signaling |
| Tri-Methyl-Histone H3 (Lys9) (D4W1U) Rabbit mAb | 13969 | Cell Signaling |
| Tri-Methyl-Histone H3 (Lys27) (C36B11) Rabbit mAb | 9733 | Cell Signaling |
| Histone H3 (D1H2) XP® Rabbit mAb | 4499 | Cell Signaling |
| Pyronin Y | 92-32-0 | Sigma-Aldrich |
| APC anti-BrdU Antibody | 364114 | BioLegend |
| MitoSOX™ Red Mitochondrial Superoxide Indicator | M36008 | Invitrogen™ |
| Carboxy-H2DFFDA | C13293 | Invitrogen™ |
| 7-AAD Viability Staining Solution | 420404 | BioLegend |

**Supplemental Table 3. Immunoblot antibodies**

| Name | Cat# | Vendor |
|---|---|---|
| SDHB Antibody (FL-280) | SC-25851 | Santa Cruz |
| anti-actin | SC-47778 | Santa Cruz |

**Supplemental Table 4. RT-qPCR primers**

| Gene | primer sequences forward | primer sequences reverse |
|---|---|---|
| Sdhb | ATTTACCGATGGGACCCAGAC | GTCCGCACTTATTCAGATCCAC |
| Sdhd | TGGTCAGACCCGCTTATGTG | GGTCCAGTGGAGAGATGCAG |
| Ifng | ATGAACGCTACACACTGCATC | CCATCCTTTTGCCAGTTCCTC |
| Il17a | TTTAACTCCCTTGGCGCAAAA | CTTTCCCTCCGCATTGACAC |
| Il17f | TGCTACTGTTGATGTTGGGAC | AATGCCCTGGTTTTGGTTGAA |
| Il22 | ATGAGTTTTTCCCTTATGGGGAC | GCTGGAAGTTGGACACCTCAA |
| Hif1a | AGCTTCTGTTATGAGGCTCACC | TGACTTGATGTTCATCGTCCTC |
| Tubulin | TTCTGGTGCTTGTCTCACTGA | CAGTATGTTCGGCTTCCCATTC |
| Gata2 | CACCCCGCCGTATTGAATG | CCTGCGAGTCGAGATGGTTG |
| Runx2 | AACGATCTGAGATTTGTGGGC | CCTGCGTGGGATTTCTTGGTT |
| Tbx6 | ATGTACCATCCACGAGAGTTGT | GGTAGCGGTAACCCTCTGTC |
| Zeb2 | ATTGCACATCAGACTTTGAGGAA | ATAATGGCCGTGTCGCTTCG |
| Kif4 | AGGTGAAGGGGATTCCCGTAA | AAACACGCCTTTTATGAGTGGA |
| Spib | AGGAGTCTTCTACGACCTGGA | GAAGGCTTCATAGGGAGCGAT |
| Ebf1 | GCATCCAACGGAGTGGAAG | GATTTCCGCAGGTTAGAAGGC |
| Mef2c | GTCAGTTGGGAGCTTGCACTA | CGGTCTCTAGGAGGAGAAACA |
| Bhlhe41 | TGTGTAAACCCAAAAGGAGCTT | TGTTCGGGCAGTAAATCTTTCAG |
| Rorc | CGCGGAGCAGACACACTTA | CCCTGGACCTCTGTTTTGGC |
| Prdm1 | TTCTCTTGGAAAAACGTGTGGG | GGAGCCGGAGCTAGACTTG |
| Irf4 | TCCGACAGTGGTTGATCGAC | CCTCACGATTGTAGTCCTGCTT |
| Stat3 | CAATACCATTGACCTGCCGAT | GAGCGACTCAAACTGCCCT |
| Batf | CTGGCAAACAGGACTCATCTG | GGGTGTCGGCTTTCTGTGTC |
| Bach1 | TGGTGAGAGTGCGGTATTTGC | GTCAGTCTGGCCTACGATTCT |

**Supplemental Table 5. ChIP-qPCR primers**

| Gene | primer sequences forward | primer sequences reverse |
|---|---|---|
| Prdm1 | TCTGGTTCCTTACCAAGGTCG | GTGGACTGGGTGGACATGAG |